Polymer Chemistry

Accepted Manuscript

This is an *Accepted Manuscript*, which has been through the Royal Society of Chemistry peer review process and has been accepted for publication.

Accepted Manuscripts are published online shortly after acceptance, before technical editing, formatting and proof reading. Using this free service, authors can make their results available to the community, in citable form, before we publish the edited article. We will replace this *Accepted Manuscript* with the edited and formatted *Advance Article* as soon as it is available.

You can find more information about *Accepted Manuscripts* in the Information for Authors.

Please note that technical editing may introduce minor changes to the text and/or graphics, which may alter content. The journal's standard Terms & Conditions and the Ethical guidelines still apply. In no event shall the Royal Society of Chemistry be held responsible for any errors or omissions in this *Accepted Manuscript* or any consequences arising from the use of any information it contains.

ROYAL SOCIETY OF CHEMISTRY

www.rsc.org/polymers

Cite this: DOI: 10.1039/c0xx00000x

www.rsc.org/xxxxxx

ARTICLE TYPE

Far-Red/Near-Infrared Fluorescent Conjugated Polymer Nanoparticles with Size-Dependent Chirality and Cell Imaging Applications†

Chunhui Dai,[a] Dongliang Yang,[b] Wenjie Zhang,[a] Biqing Bao,[b] Yixiang Cheng*[a] and Lianhui Wang*[b]

Received (in XXX, XXX) Xth XXXXXXXXX 20XX, Accepted Xth XXXXXXXXX 20XX
DOI: 10.1039/b000000x

ABSTRACT: A novel chiral conjugated polymer is developed and used for the preparation of conjugated polymer nanoparticles (CPNs) with particle sizes ranging from 80 to 190 nm. The size-dependent optical properties of chiral CPNs are fully studied and it was found that the nanoparticles exhibited a prominent red shift both in UV-vis and fluorescence with increasing diameters. The circular dichroism (CD) spectra and anisotropy *r* values of the CPNs display size-tunable chirality feature, which can be attributed to the nature of the aggregates as nanoparticles grow. Meanwhile, the obtained CPNs can serve as efficient far-red/near-infrared (FR/NIR) fluorescent probes with low cytotoxicity and high photostability for HeLa cell imaging.

Received (in XXX, XXX) Xth XXXXXXXXX 20XX, Accepted Xth XXXXXXXXX 20XX
DOI: 10.1039/b000000x

Introduction

Chiral molecules play an important role in numerous industrial and biological processes. For example, chiral drugs may exhibit different pharmacological effects because the proteins to which they bind are also chiral.[1] Moreover, chiral molecules can absorb and emit left or right circularly polarized light (CPL), which make them highly desirable candidates for CPL-active materials and have a huge potential application for luminescent materials.[2] As the evolution of nanoscience, chirality at the nanoscale has advanced significantly in the past few years, many works have been devoted to the development of chiral nanomaterials for practical applications, such as asymmetric catalysis,[3] separation technique,[4] biomolecular sensing,[5] cell imaging,[6] optoelectronic devices,[7] and so on. Recently, encouraged by application significance, more and more reports have been focused on size-dependent optical properties of chiral nanoparticles.[8] For example, Yao's group developed several organic nanoparticles with different sizes from chiral binaphthyl derivatives and studied their size-tunable photophysical properties. They found that the exciton chirality and the fluorescence emission of the particles showed size-tunable behaviors, which can be attributed to the change of dihedral angle as nanoparticles form.[9] Gil Markovich and colleagues prepared chiral penicillamine-capped CdS and CdSe quantum dots (QDs) with ultrasmall sizes (~ 3 nm) and found that the circular dichroism (CD) peaks of nanoparticles experienced red shifts and the Cotton effect intensities decreased as the increase of particles size.[10] The size-dependent CD absorption of QDs were further confirmed by Tang' work. They obtained CdTe QDs stabilized by (D, L)-GSH with different sizes (2.7–4.2 nm). The CD absorption peaks of D-/L-GSH-stabilized CdTe QDs with opposite signs in the range of 400–700 nm showed gradual bathochromic shifts, and the signals decrease when the sizes of QDs increase.[11]

Conjugated polymer nanoparticles (CPNs) are emerging as multifunctional nanoscale materials with unique photophysical properties, such as high fluorescent quantum yields, excellent photostability against photobleaching, and tunable multicolor emissions, *etc*. However, unlike semiconducting quantum dots (Qdots), CPNs show low cytotoxicity.[12] Their good biocompatibility make them excellent materials for bioimaging,[13] drug delivery,[14] and tumor therapy.[15] More importantly, some well-designed CPNs can exhibit far-red/near-infrared (FR/NIR) fluorescence (650–900 nm) with high brightness. It is well known that far-red/near-infrared (FR/NIR) fluorescent probes are desirable for biological application. This kind of probes can effectively reduce fluorescence background to reach high tissue penetration. Therefore, these far-red/near-infrared (FR/NIR) fluorescent probes are extremely promising imaging agents for non-invasive biological imaging.[13c, 13d, 16] CPNs can be fabricated by simply physical approach such as mini-emulsion, reprecipitation, encapsulation, *etc*.[17] It is possible to prepare CPNs in desired sizes by a simple reprecipitation method, which will facilitate the research on size-dependent optical properties of nanoparticles. To the best of our knowledge, very few works on size-dependent chirality of CPNs were reported. Although studies

† Electronic supplementary information (ESI) available: Synthesis of key intermediates and ^{1}H NMR spectra of chiral conjugated polymer.

[a]Key Lab of Mesoscopic Chemistry of MOE, School of Chemistry and Chemical Engineering, Nanjing University, Nanjing 210093, China. E-mail: yxcheng@nju.edu.cn.
[b]Key Laboratory for Organic Electronics and Information Displays and Institute of Advanced Materials, Nanjing University of Posts and Telecommunications, Nanjing 210023, China. E-mail: iamlhwang@njupt.edu.cn. Fax: +86-25-8586-6396.

have shown that the size-dependent optical properties of CPNs are related to the conformational changes of the polymers and the nature of the nanoparticle aggregates,[17b] the changes of chirality in CPNs still remains an interesting issue to explore.

In order to well understand size-dependent optical properties of chiral conjugated polymer nanoparticles and interactions between polymer chains, in this contribution, we have designed and synthesized a novel chiral conjugated polymer by employing a donor-acceptor strategy to produce efficient intermolecular /intramolecular energy transfer (Scheme 1). PFBOPHY units as energy acceptors and PFDBT units as energy donors were incorporated into the polymer backbone. The resulting chiral conjugated polymer, poly[9,9-di((*S*)-2-methylbutyl)fluorene)-*co*-bis(difluoroboron)1,2-bis((1*H*-pyrrol-2-yl)methylene)hydrazine-*co*-4,7-di(thiophen-2-yl)-2,1,3-benzothiadiazole(PFBOPHYDBT), was used to further prepare CPNs with different sizes by reprecipitation method. This paper discusses the size-dependent optical properties of obtained CPNs based on UV-vis, fluorescence, as well as CD, anisotropy spectroscopic analysis. Meanwhile, the CPNs (d = 80 nm) were successfully used for cell imaging because of their far-red/near-infrared fluorescence emission, high photostability and low cytotoxicity.

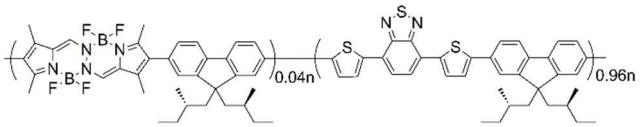

Scheme 1 Chemical structure of the chiral conjugated polymer (PFBOPHYDBT).

Experimental

Measurements and materials

NMR spectra were obtained using a 300-Bruker for ^{1}H NMR and 75 MHz for ^{13}C NMR and reported as parts per million (ppm) from the internal standard TMS. Fluorescence spectra were obtained using a RF-5301PC spectrometer. CD spectrum were determined with a Jasco J-810 spectropolarimeter. UV-vis absorption spectra were obtained using a Perkin-Elmer Lambda 35 spectrophotometer. Mass spectra (MS) were determined on a Micromass GC-TOF (EI). C, H and N of elemental analyses were performed on an Elementar Vario MICRO analyzer. Molecular weight of the polymer was determined by GPC with Waters-244 HPLC pump and THF was used as solvent and relative to polystyrene standards. The particle size distributions of CPNs were measured by dynamic light scattering (DLS) using a particle size analyser (BI-200SM, Brookhaven instruments Corp., Holtsville, NY). The morphology of the CPNs was characterized on field emission scanning electron microscope (FESEM, Hitachi, S-4800) at an accelerating voltage of 3.0 kV. The nanoparticles suspension sample for SEM measurement was dropped onto silicon slice, surface morphology was evaluated after the water evaporation. The pulse laser illumination apparatus (power: 5 mW) was purchased from Fuzhen technology Corp., Shenzhen, China. Confocal laser scanning microscope images of CPNs were taken on an Olympus Fluo-view 1000. Fluorescence quantum yield was determined using Rhodamine B in methanol (70%) as the standard. The absorbance of the solutions was kept below 0.1 to avoid internal filter effect. All experiments were performed under ambient conditions in air. The histogram of the particle height was calculated using OriginPro 9.0 software. 2,4-dimethylpyrrole, boron trifluoride etherate, thiophen-2-ylboronic acid, 4,7-dibromobenzo[*c*][1,2,5]thiadiazole, bis(pinacolato)diboron and 3-(4,5-dimethylthiazol-2-yl)-2,5-diphenyl tetrazolium bromide (MTT) were purchased from energy-chemical Co. Ltd and used without further purification. Milli-Q Water (18.2 M) was used to prepare the buffer solutions from the 10×PBS stock buffers. PBS contains NaCl (137 mM), KCl (2.7 mM), Na_2HPO_4 (10 mM) and KH_2PO_4 (1.8 mM). 2,2'-(9,9-bis((*S*)-2-methylbutyl)-9*H*-fluorene-2,7-diyl)bis(4,4,5,5-tetramethyl-1,3,2-dioxaborolane) (**M1**),[18] diiodo substituted 5,5,12,12-tetrafluoro-1,3,8,10-tetramethyl-5,12-dihydropyrrolo[1,2-*d*]pyrrolo[1',2':4,5][1,2,4,3]triazaborinino[2,1-*a*][1,2,4,3]triazaborinine-6,13-diium-5,12-diuide (**M2**),[19] and 4,7-bis(5-bromothiophen-2-yl)benzo[*c*][1,2,5]thiadiazole (**M3**),[20] were prepared according to the procedure described in the literature.

Monomer and polymer synthesis

Synthesis of M1

A mixture of 2,7-dibromo-9,9-bis((*S*)-2-methylbutyl)-9*H*-fluorene (742.8 mg, 1.6 mmol) and bis(pinacolato)diboron (1.22 g, 4.8 mmol) was added in Schlenk tube. 16 mL of anhydrous DMSO was added by syringe after the tube was evacuated under vacuum and flushed with Ar three times. After the mixture was dissolved by heating, KOAc (470 mg, 4.8 mmol) and [$PdCl_2$(dppf)] (40 mg, 0.055 mmol) were added. The reaction mixture was stirred for 15 h at 65 °C under Ar atmosphere. After cooling down to room temperature, 150 mL of water was added and gray solids were obtained by filtration. The residue was purified by column chromatography on silica gel (petroleum ether/ethyl acetate, v/v, 30:1) to give the product (R_f = 0.5) as a white solid (455.7 mg, 51%). ^{1}H NMR (300 MHz, $CDCl_3$): δ 7.83–7.78 (m, 4H, ArH), 7.73–7.71 (d, 2H, ArH), 2.15–2.06 (m, 2H, CH_2), 1.96–1.86 (m, 2H, CH_2), 1.38 (s, 24H, CCH_3), 0.88–0.63 (m, 6H, $CHCH_2$), 0.62–0.50 (m, 6H, CH_3), 0.23–0.17 (m, 6H, CH_2CH_3); ^{13}C NMR (75 MHz, $CDCl_3$): δ 150.4, 143.8, 133.5, 130.1, 119.3, 83.5, 77.3, 76.9, 76.5, 47.4, 30.9, 30.5, 24.7, 20.7, 10.7; MS (EI, *m/z*): 558.4 (M^+); anal. calcd for $C_{35}H_{52}B_2O_4$: C, 75.28; H, 9.39. Found: C, 75.11; H, 9.53%.

Synthesis of M2

Iodic acid (352 mg, 2.0 mmol) dissolved in a minimal amount of water was added dropwise to a solution of **6** (338 mg, 1.0 mmol) and iodine (316 mg, 2.5 mmol) in 150 mL ethanol. The resulting mixture was stirred at 60 °C for 3 h. After cooling to room temperature, the yellow precipitate was collected by filtration and further recrystallized from ethanol for three times to afford **M2** as a yellow solid (520 mg, 88%). ^{1}H NMR (300 MHz, $CDCl_3$): δ 8.00 (s, 2H, CH), 2.55 (s, 6H, CH_3), 2.31 (s, 6H, CH_3); ^{13}C NMR (75 MHz, $CDCl_3$): δ 142.6, 134.1, 76.4, 75.9, 75.5, 14.1, 12.5; MS (EI, *m/z*): 589.7 (M^+); anal. calcd for $C_{14}H_{14}B_2F_4I_2N_4$: C, 28.36; H, 2.54; N, 9.31. Found: C, 28.51; H, 2.39; N, 9.50%.

Synthesis of the chiral conjugated polymer

A mixture of **M1** (111.7 mg, 0.20 mmol), **M2** (4.72 mg, 0.008 mmol), **M3** (88.0 mg, 0.192 mmol) and [$Pd(PPh_3)_4$] (10 mg, 0.0086 mmol) was added in a 50 mL Schlenk tube. 2 drops of Aliquat 336, 10 mL of Na_2CO_3 aqueous solution (2 mol/L), and 15 mL of toluene added by syringe after the tube was evacuated and refilled with Ar three times. The mixed solution was stirred at 80 °C for 24 h under Ar atmosphere. After cooling, the reaction mixture was extracted with ethyl acetate. The organic phases were combined and dried over anhydrous $MgSO_4$. The solvent

was removed under reduced pressure. The resulting residue was dissolved in a small quantity of THF. The resulting mixture was added into 50 mL of methanol to precipitate the polymer. The polymer was collected as a dark red solid (100.7 mg). Yield: 83%. $[\alpha]_D^{25}$ = +850.0 (*c* 1.0, $CHCl_3$); GPC results: M_w = 11760, M_n = 24310, PDI = 2.05. ^{1}H NMR (300 MHz, $CDCl_3$): δ 8.17–8.09 (m, 1H), 7.95–7.87 (m, 1H), 7.78–7.46 (m, 6H), 2.25–1.98 (m, 3H), 1.61 (s, 9H), 1.40–1.38 (d, 1H), 1.26 (s, 6H), 1.10 (s, 20H), 0.88–0.77 (m, 11H).

Preparation and characterization of CPNs

The CPNs were prepared *via* the precipitation method according to the reported method.[13g] The chiral conjugated polymer was first dissolved in anhydrous THF to make a 100 mg/L (100 ppm) stock solution. After stirring overnight at room temperature, the obtained polymer solutions were further diluted to 10, 20, and 50 ppm in THF, respectively. The solution was filtered with a 0.22 μm syringe filter. A 2 mL quantity of the polymer solution was injected rapidly into 8 mL Milli-Q Water under sonication. The dilute CPNs suspension was obtained after THF evaporation under reduced pressure. The CPNs suspension was further concentrated to 2 mL and purified with a syringe filter (0.22 μm or 0.45 μm) to obtain the CPNs suspension with different sizes. The concentrations of CPNs suspension with various sizes were adjusted to ~ 20 ppm by diluting with Milli-Q water and used for optical properties investigation.

Cell culture

HeLa cells were cultured in Dulbecco's modified Eagle's medium (DMEM) containing 10% fetal bovine serum (FBS) and antibiotics (100 U/mL penicillin and 100 μg/mL streptomycin), maintained at 37 °C in a humidied atmosphere of 95% air and 5% CO_2. The cells were pre-cultured prior to experiments until confluence was reached. For confocal imaging, the cell suspension was placed on a 15-mm-diameter chamber, and cultured until the density reached confluence for fluorescence imaging.

Photostability of CPNs

The photostability of CPNs was evaluated by monitoring their respective fluorescence intensity changes after pulse laser irradiation (excition at 532 nm) for different time periods. At the designated time intervals, the fluorescent emission intensity of the NP suspension was measured with the spectrometer, and was further expressed by I/I_0, where I_0 is the fluorescent intensity at 660 nm (d = 80 nm) of fresh NPs suspension and I is that of CPNs after irradiation.

Cytotoxicity assay

The cytotoxicity of CPNs (d = 80 nm) against HeLa cells was evaluated by MTT assay. In brief, HeLa cells were seeded in 96-well plates (Costar, IL, USA) at an intensity of 4×10^4 cells mL^{-1}. After 24 h incubation, the cells were exposed to a series of doses of CPNs with the concentration of 0, 5, 10, 20, 40 ppm and further cultured at 37 °C. After 48 h, the sample wells were washed twice with 1×PBS buffer and 100 μL of freshly prepared MTT (0.5 mg/mL) solution in culture medium was added into each sample well. The MTT medium solution was carefully removed after 3 h incubation in the incubator for the sample wells, whereas the control wells without addition of MTT solution were washed twice with 1×PBS buffer. DMSO (150 μL) was then added into each well and the plate was gently shaken for 10 min at room temperature to dissolve all the precipitates formed. The absorbance of individual wells at 570 nm was then monitored by the microplate Reader (BioTek, PowerWave XS2, Vermont, USA). The absorbance of MTT in the sample well was determined by the differentiation between the absorbance of the sample well and that of the corresponding control well. Cell viability was expressed by the ratio of the absorbance of MTT in the sample wells to that of the cells incubated with culture medium only.

Cellular imaging

HeLa cells were seeded into confocal imaging chambers at a density of 1×10^5 per dish and incubated overnight at 37 °C. Then the medium was removed and the adherent cells were washed twice with 1×PBS buffer. The CPNs suspension at the concentration of ~ 3 ppm was then added to the chamber. After incubation for 2 h, the cells were washed three times with 1×PBS buffer and then the cellular images were recorded by confocal laser scanning microscope (Olympus Fluo-view 1000, Japan) at 559 nm with a 650 nm longpass barrier filter.

Results and discussion

Monomers and chiral conjugated polymer synthesis

The synthetic routes to the monomers and the chiral conjugated polymer are shown in Scheme 2. The monomer **M1** was obtained by two synthetic steps from the starting material of 2,7-dibromo-9*H*-fluorene (**1**). The intermediate 2,7-dibromo-9,9-bis((*S*)-2-methylbutyl)-9*H*-fluorene (**2**) was synthesized in 63% yield through the alkylation reaction of 2,7-dibromo-9*H*-fluorene (**1**) and (*S*)-1-bromo-2-methylbutane with potassium *t*-butoxide as base in DMF at 40 °C for 35 min.[18a] Suzuki-Miyaura reaction between **2** and bis(pinacolato)diboron in the presence of potassium acetate and $[Pd(dppf)Cl_2]$ in anhydrous DMSO at 65 °C for 15 h afforded 2,2'-(9,9-bis((*S*)-2-methylbutyl)-9*H*-fluorene-2,7-diyl)bis(4,4,5,5-tetramethyl-1,3,2-dioxaborolane) (**M1**) in 51% yield.[18b] The monomer **M2** was prepared by four reaction steps from 2,4-dimethyl-1*H*-pyrrole (**3**). 3,5-dimethyl-1*H*-pyrrole-2-carbaldehyde (**4**) was obtained by the Vilsmeier-Haack reaction of 2,4-dimethylpyrrole (**3**) with phosphorus oxychloride in DMF at room temperature for 1.5 h in 75% yield. Condensation of the aldehyde with hydrazine hydrate in ethanol solution gave a Schiff base (**5**). 5,5,12,12-tetrafluoro-1,3,8,10-tetramethyl-5,12-dihydropyrrolo[1,2-*d*]pyrrolo[1',2':4,5][1,2,4,3]triazaborinino[2,1-*a*][1,2,4,3]triazaborinine-6,13-diium-5,12-diuide (**6**) was prepared in a one-pot BF_2 chelation reaction. The monomer **M2** was synthesized in 88% yield via iodination of BOPHY (**6**) in the presence of iodine and iodic acid at 60 °C for 3 h. The monomer **M3** was prepared in 52% yield by bromination of 4,7-di(thiophen-2-yl)benzo[*c*][1,2,5]thiadiazole (**9**), which was obtained by a Suzuki coupling between thiophen-2-ylboronic acid (**7**) and 4,7-dibromobenzo[*c*][1,2,5]-thiadiazole (**8**). The chiral conjugated polymer could be obtained by $[Pd(PPh_3)_4]$-catalyzed Suzuki polycondensation reaction of **M1**, **M2** and **M3** in toluene and Na_2CO_3 aqueous mixture at 80 °C over 24 h (83% yield). Herein, molar ratio of **M1**, **M2** and **M3** in the main chain backbone of the chiral polymer is 1.0: 0.04: 0.96. The resulting chiral copolymer has a number average molecular weight (M_n) of 24310 and a weight average molecular weight (M_w) of 11760 with a poly-dispersity index (PDI) of 2.05, which was determined by gel permeation chromatography (GPC) using THF as eluent and polystyrene as standard. The chemical structures of the monomers **M1**, **M2**, **M3** and the chiral polymer were characterized by ^{1}H NMR and ^{13}C NMR. The chiral polymer is soluble in common organic solvents, such as tetrahydrofuran, ethyl acetate, toluene, and dichloromethane, which can be

attributed to the flexible alkyl side chain on the fluorene unit.

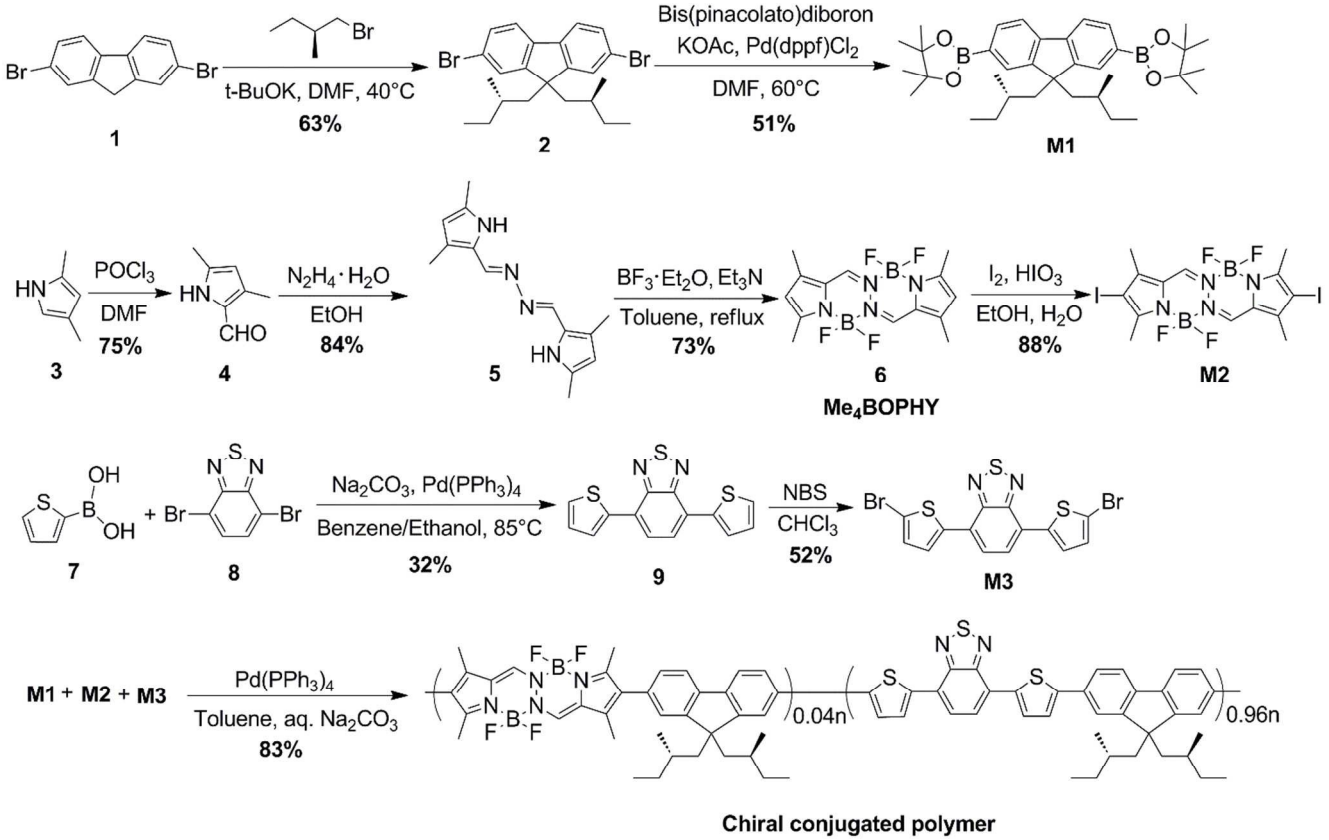

Scheme 2 Synthetic procedures for **M1**, **M2**, **M3** and the chiral conjugated polymer.

Preparation and characterization of CPNs

CPNs were prepared via precipitation method similar to the reported literature procedure.[13e] The preparation procedure involves a rapid mixing of a dilute solution of polymer dissolved in a "good" solvent with an excess of water (''poor'' solvent to the polymer) under ultrasonication. The rapid mixing with water leads to a sudden decrease in solvent quality and the significant change of solvent polarity, resulting in the formation of a suspension of conjugated polymer nanoparticles (CPNs). The particle size is dependent on the starting concentration of the conjugated polymer in "good" organic solvents.[12a, 17a] Herein, we prepared a series of CPNs with different sizes using the starting concentrations of the chiral polymer solutions in THF of 10, 20, and 50 ppm, respectively. The obtained dark red nanoparticle suspension was slightly turbid as evidenced by light scattering. The diameters of the CPNs are characterized by using dynamic light scattering (DLS) and imaged using scanning electron microscopy (SEM) as shown in Fig. 1. The average hydrodynamic diameters of CPNs are ~ 91 nm, ~ 132 nm, and ~ 200 nm, respectively (Fig.1 (d-f)). The FESEM images of the CPNs are spherical in shape, and the average sizes are ~ 80 nm, ~ 120 nm, and ~ 190 nm, respectively (Fig.1 (a-c)).

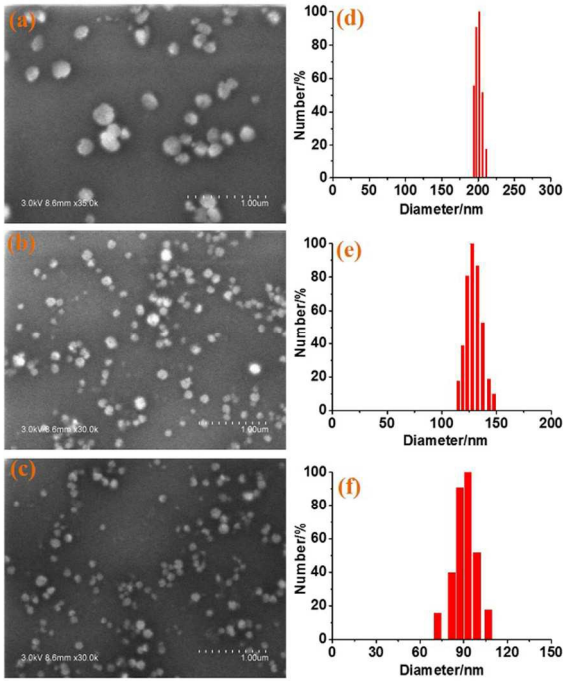

Fig. 1 FESEM images of CPNs (a-c) and histograms of the size distribution (measured by DLS) (d-f).

Optical properties of CPNs and chiral polymer in dilute THF solution

The UV-vis absorption spectra of the CPNs dispersions with different sizes and the chiral polymer (20 ppm corresponding to

9,9-bis((*S*)-2-methylbutyl)-9*H*-fluorene moiety) in dilute THF solution are shown in Fig. 2. As shown in Fig. 2, the absorption band of the chiral polymer in THF solution exhibits strong absorption maxima at 380 nm and 530 nm, respectively. The longer absorption band of the conjugated polymer is attributed to intramolecular charge transfer (ICT) between the electron-rich donor and the electron-deficient acceptor. Compared with the chiral polymer in THF solution, the absorption peaks of CPNs around 380 nm became shoulder peaks and emerged additional peaks centered at ~ 551 nm, which experienced a weak red-shift as the particle size increases from 80 to 190 nm. The size-dependent red-shift of CPNs is probably related to the formation of nanoparticle aggregates, which enhanced inter- and intrachain interactions.[9b, 17a]

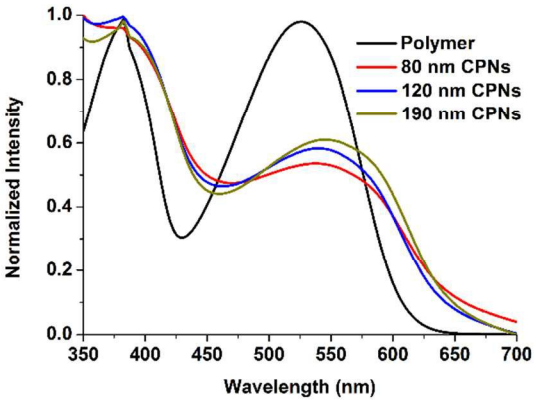

Fig. 2 UV/vis absorption spectra of CPNs dispersions with different sizes and the chiral polymer in dilute THF solution (20 ppm).

Fig. 3(a) presents the CD spectra of CPNs and the chiral polymer in dilute THF solution. As evidenced from Fig. 3(a), the chiral polymer displays a bisignated Cotton effect with a positive wave situated at around 356 nm and a negative wave at 406 nm. It is interesting to note that the intensities of CD signals show gradual decrease as the nanoparticle sizes increase from 80 to 190 nm, meanwhile, all the CD peaks experience bathochromic shifts to low energy side as the increase of nanoparticles size, which is due to the enhanced interactions between polymer chains.[9b]

To further investigate the size-tunable chirality behaviors of CPNs, in this paper, we explored the steady-state emission anisotropy spectra of CPNs and the chiral polymer in dilute THF solution through the emission bands (Fig. 3(b)). The fluorescent polarization feature could be normally evaluated by the anisotropy r value, which can be defined as $r = (I_{\parallel}-I_{\perp})/(I_{\parallel}+I_{\perp})$, where $I_{\parallel}$ and $I_{\perp}$ are the photoluminescence intensity measured in the planes parallel and perpendicular to the excitation radiation, respectively.[21] Herein, we carried out the steady-state emission anisotropy spectra of CPNs dispersions with different sizes and the chiral polymer in dilute THF solution at 665 nm of the emission band (excitation at 540 nm). As is evident from Figure 3(b), there are obvious different luminescence polarization between CPNs dispersions with different sizes and the chiral polymer in dilute THF solution. The chiral polymer shows a weak luminescence polarization signal (r = 0.040), which is smaller than that of CPNs. Meanwhile, the anisotropy r values of CPNs show the gradual enhancement from ~ 0.075 to ~ 0.120 as the increase of nanoparticle size, which may be related to the limitation of the free motion of the chiral conjugated polymer. When the conjugated polymer collapse into sphere and grow, the limitation of rotational moment become stronger, which leads to a lower rotational diffusion and thus a larger fluorescence anisotropy value.[22]

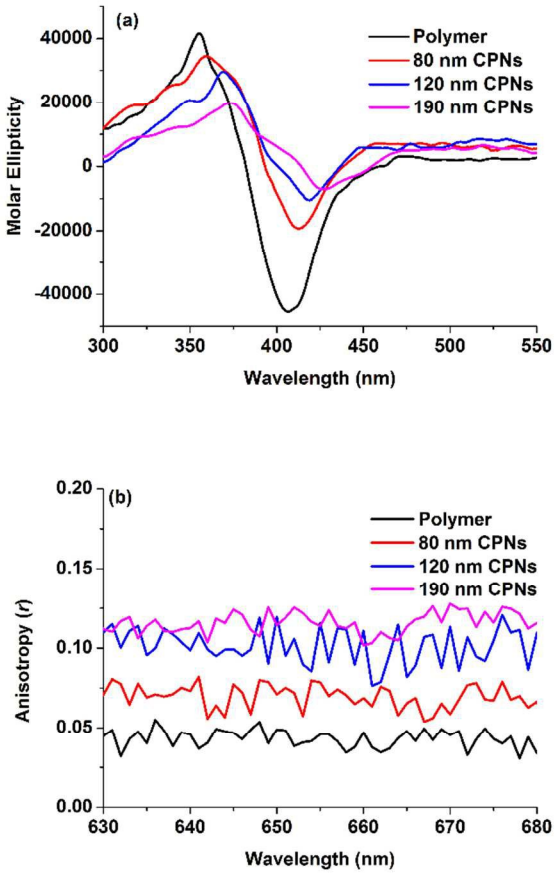

Fig. 3 CD spectra (a) and anisotropy spectra (b) of CPNs and the chiral polymer in dilute THF solution (20 ppm).

Fig. 4 displays the fluorescence emission spectra of CPNs with various mean diameters and the chiral conjugated polymer in dilute THF solution (excited at 540 nm). The chiral conjugated polymer in THF solution exhibits a strong fluorescence centered at ~ 642 nm, and the quantum yield is 0.43. The maxima emission peaks of CPNs appear at about 665 nm with a red shift as high as 23 nm, which is likely because the intramolecular interactions of chain-chains become strong when the polymer chains are collapsed into a spherical particle.[17a] The excitons on high-energy segments undergo rapid energy transfer to lower-energy segments, therefore, all the fluorescence emission of CPNs comes from low energy level. However, the conjugated polymer in dilute THF solution shows a weak interaction between chains and lacks low-energy sites for singlet excitons, which leading to a shorter-wavelength emission compared to CPNs suspension.[23, 24] In addition, the fluorescence emission wavelength appears a little red shifted from 660 to 671 nm as the size of the CPNs increase, which is related to the enhanced interaction between polymer chains as the nanoparticles grow. Meanwhile, thiophene units in the polymer backbone here may result in the distorted polymers conformations according to Hiroshi Masuhara's report.[8d] The distorted conformations of the polymer may lead to lattice softening and weaken the intermolecular interaction. Herein, we think that the size-dependent red-shift is related to energy level transition, which can be regarded as the cooperative result of the enhanced interactions of chain-chains and the distorted

conformations of the polymer.

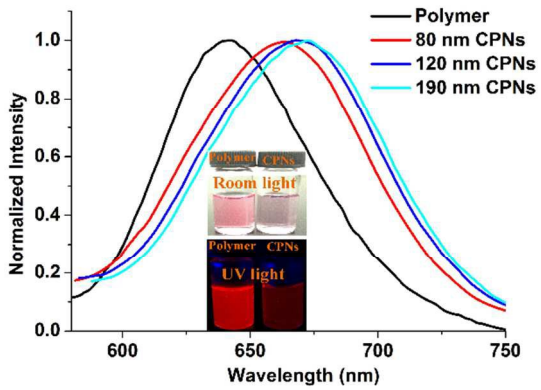

Fig. 4 Fluorescence emission spectra of CPNs with different sizes and chiral polymer in dilute THF solution (20 ppm). The excitation wavelength is at 540 nm.

In this paper, we further investigated the application of CPNs as fluorescence bioimaging probes. Because of the highest quantum yields and smallest diameter, the nanoparticles with the diameter of 80 nm (quantum yield: 9%) were employed for HeLa cell imaging. It is well known that good photostability is of great importance for biological application. Photostability evolutions of CPNs were carried out under continuous laser scanning upon excitation at 532 nm with a fixed pulse laser illumination apparatus (power: 5 mW). As is demonstrated in Fig. 5, CPNs exhibit only ~ 7% decrease in PL intensity after 10 min of continuous irradiation, indicating that these CPNs possess high photostability and can act as the desirable fluorescence probes for bioimaging applications.

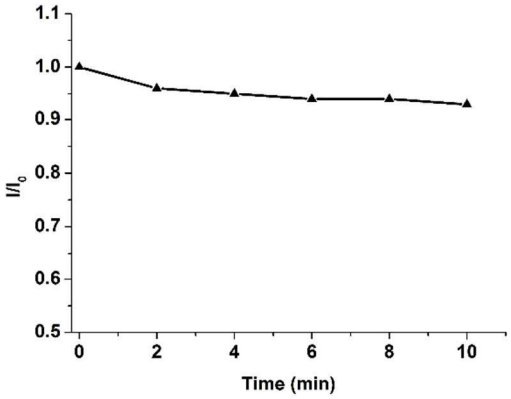

Fig. 5 Photostability of CPNs (d = 80 nm) upon continuous laser excitation at 532 nm for 0-10 min. I_0 is the initial fluorescence intensity at 660 nm for the fresh CPNs suspension, I is the fluorescence intensity after radiation at different time points.

The cytotoxicity of CPNs (d = 80 nm) against HeLa cells was estimated by MTT assays. Fig. 6 shows the cell viability after incubation with the fresh CPNs at concentrations of 5, 10, 20 and 40 ppm for 48 h, respectively. It is worth noting that CPNs shows low cytotoxicity even at 40 ppm after 48 h, demonstrating that this kind of CPNs can be used as safe fluorescence probes for live cell bioimaging.

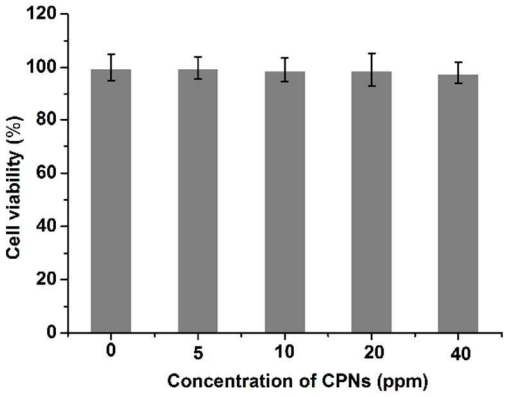

Fig. 6 Metabolic viability of HeLa cells after incubation with CPNs suspension (d = 80 nm) at different concentrations for 48 h.

The applications of CPNs in cellular imaging were studied by confocal laser scanning microscopy with HeLa cells. After incubation with the CPNs suspensions (~ 3 ppm) at 37 °C for 2 h, HeLa cells were stained. The confocal images were taken upon excitation at 559 nm with a 650 nm longpass barrier filter. Fig. 7 presents the confocal images of HeLa stained with CPNs suspension. It is clearly found that CPNs were taken up by HeLa cells and the fluorescence dots accumulated in the edge of cytoplasm.

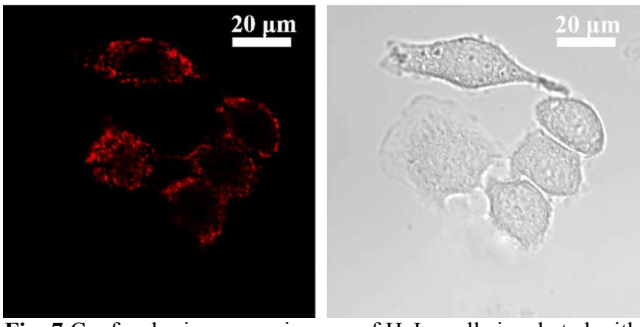

Fig. 7 Confocal microscopy images of HeLa cells incubated with CPNs (d = 80 nm) for 2 h, upon excitation at 559 nm. (a) Excited with 559 nm laser; (b) Bright field image.

Conclusions

In this study, we prepared a series of novel chiral far-red/near-infrared fluorescent CPNs with different sizes ranging from 80 nm to 190 nm by using the reprecipitation method. These BOPHY-containing CPNs show size-dependent chirality with different nanoparticles diameters, which can help us understand the interaction mechanism between polymer chains and size-dependent optical properties of chiral conjugated polymer nanoparticles. Meanwhile, due to their far-red/near-infrared (FR/NIR) emission, high photostability, low cytotoxicity, the obtained CPNs were successfully used for live cell imaging.

Acknowledgements

This work was supported by the National Natural Science Foundation of China (21174061, 51173078, 21172106, and 21474048) and open project of Beijing National Laboratory for Molecular Sciences.

Notes and references

1 Q. Shen, L. Wang, H. Zhou, H. D. Jiang, L. S. Yu, S. Zeng, *Acta Pharmacologica Sinica*, 2013, **34**, 998.

2 (a) J. Yuasa, T. Ohno, K. Miyata, H. Tsumatori, Y. Hasegawa, and T. Kawai, *J. Am. Chem. Soc.*, 2011, **133**, 9892; (b) H. Maeda, Y. Bando, K. Shimomura, I. Yamada, M. Naito, K. Nobusawa, H. Tsumatori, and T. Kawai, *J. Am. Chem. Soc.*, 2011, **133**, 9266; (c) J. Z. Liu, H. M. Su, L. M. Meng, Y. H. Zhao, C. M. Deng, J. C. Y. Ng, P. Lu, M. Faisal, J. W. Y. Lam, X. H. Huang, H. K. Wu, K. S. Wong, and B. Z. Tang, *Chem. Sci.*, 2012, **3**, 2737.

3 (a) J. Zhang, M. T. Albelda, Y. Liu, and J. W. Canary, *Chirality*, 2005, **17**, 404; (b) G. Szollosi, A. Mastalir, Z. Kiraly and I. Dekany, *J. Mater. Chem.*, 2005, **15**, 2464; (c) A. G. Hu, G. T. Yee, and W. B. Lin, *J. Am. Chem. Soc.*, 2005, **12**, 12486; (d) S. Jansat, D. Picurelli, K. Pelzer, K. Philippot, M. Gómez, G. Muller, P. Lecante, and B. Chaudret, *New J. Chem.*, 2006, **30**, 115.

4 C. Nilsson and S. Nilsson, *Electrophoresis*, 2006, **27**, 76.

5 L. Torsi, G. M. Farinola, F. Marinelli, M. C. Tanese, O. H. Omar, L. Valli, F. Babudri, P. G. F. PalmisanoZambonin and F. Naso, *Nat. Mater.*, 2008, **7**, 412.

6 X. Yang, L. F. Gan, L. Han, D. Li, J. Wang, and E. K. Wang, *Chem. Commun.*, 2013, **49**, 2302.

7 O. B. Dor, N. Morali, S. Yochelis, L. T. Baczewski, and Y. Paltiel, *Nano Lett.*, 2014, **14**, 6042.

8 (a) H. B. Fu and J. N. Yao, *J. Am. Chem. Soc.*, 2001, **123**, 1434; (b) H. B. Fu, B. H. Loo, D. B. Xiao, R. M. Xie, X. H. Ji, J. N. Yao, B. W. Zhang, and L. Q. Zhang, *Angew. Chem. Int. Ed.*, 2002, **41**, 962; (c) D. B. Xiao, L. Xi, W. S. Yang, H. B. Fu, Z. G. Shuai, Y. Fang, and J. N. Yao, *J. Am. Chem. Soc.*, 2003, **125**, 6740; (d) N. Kurokawa, H. Yoshikawa, N. Hirota, K. Hyodo, and H. Masuhara, *ChemPhysChem*, 2004, **5**, 1609; (e) F. K. Wang, M. Han, K. Y. Mya, Y. B. Wang, and Y. Lai, *J. Am. Chem. Soc.*, 2005, **127**, 10350.

9 (a) D. B. Xiao, W. S. Yang, J. N. Yao, L. Xi, X. Yang, and Z. G. Shuai, *J. Am. Chem. Soc.*, 2004, **126**, 15439; (b) Y. L. Zhang, A. D. Peng, J. Wang, W. S. Yang, J. N. Yao, *J. Photoch. Photobio. A*, 2006, **181**, 94.

10 A. B. Moshe, D. Szwarcman, and G. Markovich, *ACS Nano*, 2011, **5**, 9034.

11 Y. L. Zhou, Z. N. Zhu, W. X. Huang, W. J. Liu, S. J. Wu, X. F. Liu, Y. Gao, W. Zhang, and Z. Y. Tang, *Angew. Chem. Int. Ed.*, 2011, **50**, 11456.

12 (a) L. H. Feng, C. L. Zhu, H. X. Yuan, L. B. Liu, F. T. Lv and S. Wang, *Chem. Soc. Rev.,* 2013, **42**, 6620; (b) J. Liu, J. L. Geng and B. Liu, *Chem. Commun.*, 2013, **49**, 149.

13 (a) K. Li and B. Liu, *J. Mater. Chem.*, 2012, **22**, 1257; (b) Y. Q. Li, J. Liu, B. Liu and N. Tomczak, *Nanoscale*, 2012, **4**, 5694; (c) J. Liu, G. X. Feng, D. Ding and B. Liu, *Polym. Chem.*, 2013, **4**, 4326; (d) D. Ding, J. Liu, G. X. Feng, K. Li, Y. Hu, and B. Liu, *Small*, 2013, **9**, 3093; (e) B. Q. Bao, N. J. Tao, D. L. Yang, L. H. Yuwen, L. X. Weng, Q. L. Fan, W. Huang, and L. H. Wang, *Chem. Commun.*, 2013, **49**, 10623; (f) L. H. Feng, L. B. Liu, F. T. Lv, G. C. Bazan, and S. Wang, *Adv. Mater.*, 2014, **26**, 3926; (g) J. Liu, J. L. Geng, L. D. Liao, N. Thakor, X. H. Gao, and B. Liu, *Polym. Chem.*, 2014, **5**, 2854.

14 X. L. Feng, F. T. Lv, L. B. Liu, H. W. Tang, C. F. Xing, Q. Yang and S. Wang, *ACS Appl. Mater. Interfaces*, 2010, **2**, 2429.

15 J. L. Geng, C. Y. Sun, J. Liu, L. D. Liao, Y. Y. Yuan, N. Thakor, J. Wang, and B. Liu, *Small*, 2014, DOI: 10.1002/smll.201402092.

16 (a) J. V. Frangioni, *Curr. Opin. Chem. Biol.*, 2003, **7**, 626; (b) J. Liu, J. L. Geng and B. Liu, *Chem. Commun.*, 2013, **49**, 1491.

17 (a) J. Pecher and S. Mecking, *Chem. Rev.*, 2010, **110**, 6260; (b) D. Tuncel, and H. V. Demir, *Nanoscale*, 2010, **2**, 484; (c) Z. Y. Tian, J. B. Yu, C. F. Wu, C. Szymanski, and J. McNeill, *Nanoscale*, 2010, **2**, 1999.

18 (a) M. S. Maji, T. Pfeifer, and A. Studer, *Chem. Eur. J.,* 2010, **16,** 5872; (b) N. Berton, F. Lemasson, N. Stürzl, F. Hennrich, M. M. Kappes, and M. Mayor, *Chem. Mater.,* 2011, **23,** 2237.

19 (a) I. Tamgho, A. Hasheminasab, J. T. Engle, and C. J. Ziegler, *J. Am. Chem. Soc.*, 2014, **136**, 562; (b) C. J. Yu, L. J. Jiao, P. Zhang, Z. Y. Feng, C. Cheng, Y. Wei, X. L. Mu, and E. H. Hao, *Org. Lett.*, 2014, **16**, 3048; (c) X. Ma, E. A. Azeem, X. L. Liu, Y. X. Cheng, and C. J. Zhu, *J. Mater. Chem. C*, 2014, **2**, 1076.

20 A. Saeki, S. Yoshikawa, M. Tsuji, Y. Koizumi, M. Ide, C. Vijayakumar, and S. Seki, *J. Am. Chem. Soc.*, 2012, **134**, 19035.

21 B. Valeur, Molecular Fluorescence: Principles and Applications, Wiley-VCH: Weinheim, 2002.

22 (a) V. Vicinelli, G. Bergamini, P. Ceroni, V. Balzani, F. Vögtle and O. Lukin, *J. Phys. Chem. B*, 2007, **111**, 6620; (b) B. Branchi, G. Bergamini, L. Fiandro, P. Ceroni, F. Vögtle and F.-G. Klärner, *Chem. Commun.*, 2010, **46**, 3571.

23 J. K. Grey, D. Y. Kim, B. C. Norris, W. L. Miller, and P. F. Barbara, *J. Phys. Chem. B*, 2006, **110**, 25568.

24 K. Sun, H. B. Chen, L. Wang, S. Y. Yin, H. Y. Wang, G. X. Xu, D. N. Chen, X. J. Zhang, C. F. Wu, and W. P. Qin, *ACS Appl. Mater. Interfaces*, 2014, **6**, 10802.

25